

## Low Operating Voltage and Small Size SPAD Design for Radiation Monitoring System in Nuclear Power Plants

Jinseok Oh<sup>a</sup>, Jungyeol Yeom<sup>a\*</sup>, Inyong Kwon<sup>b\*</sup>,

<sup>a</sup>Department of biomedical engineering, Korea University, Hana-Science Building 145 Anam-ro, Seongbuk-gu, Seoul 02841, Korea

<sup>b</sup>Korea Atomic Energy Research Institute, 111, Daedeok-daero 989 Beon-gil, Yuseong-gu, Daejeon 34057, Korea and Department of Nuclear and Radiation Safety, Korea University of Science and Technology (UST), Daejeon 34113, Korea

\*Corresponding author: [ikwon@kaeri.re.kr](mailto:ikwon@kaeri.re.kr)  
E-mail: [ohjs1027@korea.ac.kr](mailto:ohjs1027@korea.ac.kr)

### 1. Introduction

As the public's awareness of nuclear power plants increases, the international community is strengthening safety standards for severe accidents of nuclear power plants. In addition, the International Atomic Energy Agency (IAEA), on concerns about enormous industrial and economic losses caused by high radioactive leaks when severe accidents occur, is demanding the capacity to strengthen monitoring systems and environmental criteria for nuclear safety. However, most of the existing radiation monitoring systems in plants are difficult to expect normal operation in harsh environments such as high radiation and loss of power, so it is necessary to develop advanced radiation monitoring systems accordingly. Furthermore, it is capable of the sensor network system covering whole nuclear power plants through the next-generation radiation sensor as one huge sensor array, like Figure. 1.

Radiation detectors based on the semiconductor have a lot of advantages. In particular, silicon photomultiplier (SiPM) among the photo detection devices is being magnified as a high resolution, small size, low power consumption and high potential ability integrated with CMOS logics, from the past decade. Presently, it is accelerated because of the development of the Single Photon Avalanche Diodes (SPAD) for single photon imaging. With this, it is able to integrate SPADs with the readout logic in a CMOS process and obtain digitized output.

In this work, we designed SPAD under the PDK rule in a common 180 nm CMOS technology process. In order to integrate the readout circuitry, SPADs preferentially were designed and measured as single-channel. To analyze the performance of proposed SPAD design, Photon Detection Probability (PDP) and Dark count rate (DCR) was intensively measured. DCR that was primarily generated by temperature between band-to-band was classified and analyzed by the MATLAB. PDP was performed only at 405 nm, which was a target wavelength of the LYSO crystal.

### 2. Design and measurement

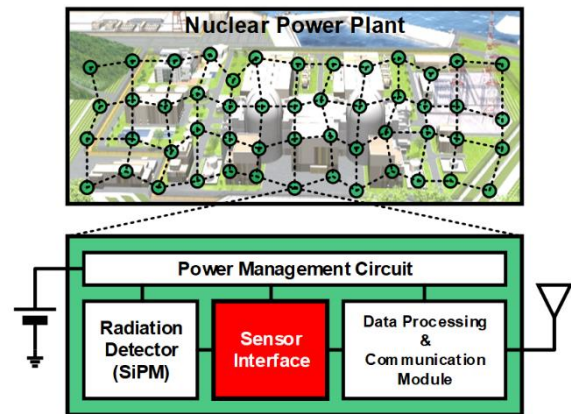


Figure. 1. Diagram of the radiation detector network covered the plant

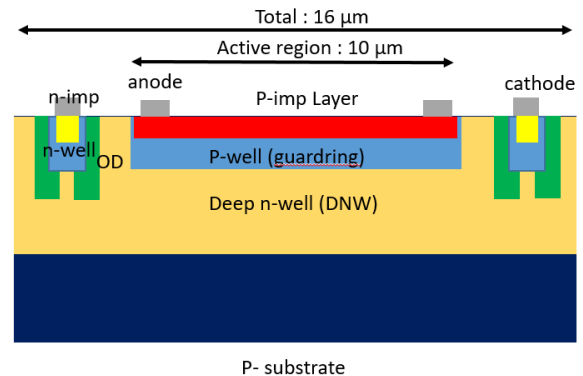


Figure. 2. Cross section of proposed SPAD design with layer information. The depletion region is created by coupling the p-well and DNW.

In this section, the design of the SPADs is explained with the technology and parameters. Additionally, the measurements are analyzed.

#### 2.1 SPAD Design

The SPADs are manufactured in a 180 nm standard CMOS technology with the P-N junction. A main part of the SPAD design is to determine the size and depth of the multiple regions [1]. According to this, each parameter can have various characteristics, in this work, some

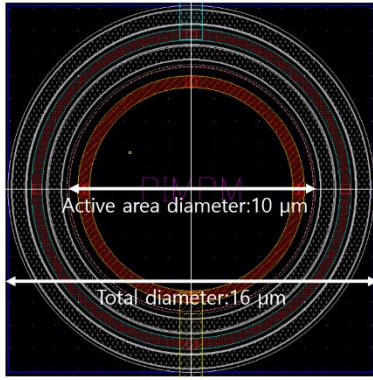


Figure 3. Single-SPAD layout with a diameter.

technology and layer characteristics were explored to be suitable for common CMOS processes and performance of the SPAD was analyzed.

The radius of the active region (AR) that is complied with the PDK rule is 5 μm. A cross-section including each layer information can be seen in Figure. 2. The depletion region corresponding to AR consists of the pwell-deep nwell (DNW), and p-imp layer is used for the top layer. A guard-ring that was constructed by STI and p well around the cathode is assigned to prevent edge breakdown and create a uniform magnetic field. Moreover, currents are simultaneously supplied through the donut type of the metal line connected to anode and cathode pin. The proposed SPAD layout can be seen in Figure. 3.

In order to operate the SPAD normally, it can be recharged through ‘quenching’ in the ‘avalanche state’, and the dead time that is to go back to the normal state varies according to the passive quenching circuit(PQC) or active quenching circuit (AQC) [2]. In this work, a 105 kΩ series resistor that is the PQC is connected to anode.

## 2.2 Breakdown voltage

To determine the operating voltage, it is necessary to preferentially check the I-V curve. The measured I-V curve was tested under the condition that the SPAD was ‘open’, which the light coming in. In Figure. 4, It can be seen that the curve rises sharply from  $V_{BD} = 10.75$  V and above.

## 2.3 Dark Count Rate set-up & measurement

DCR is the most important parameter among the noise factors of SPAD, and it must be verified because the dead time and Photon counts could be degraded by dark count. In addition, DCR is mainly caused by thermal generation caused by excess bias voltage that determines the sensitivity of SPAD, so performance can be maximized in this trade-off [3]. Therefore, DCR is measured at room temperature as regular intervals of the excess bias voltage and demonstrated with the oscilloscope. All of the pulse data are saved as Excel files, after that, each peak is selected and counted through MATLAB. The

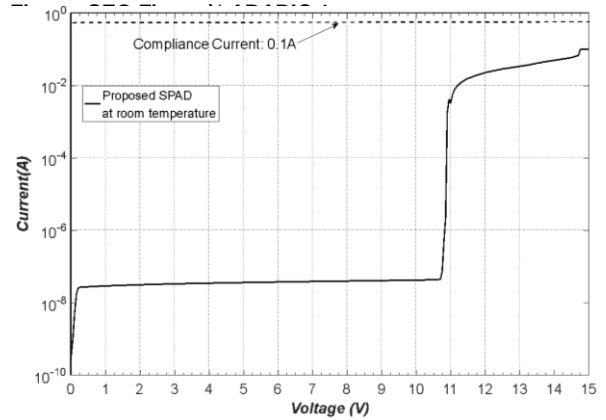


Figure 4. Log scale I-V curve as voltage swipe ranged from 0 V to 15 V. Current is limited to prevent the failure in SPAD as above compliance current.

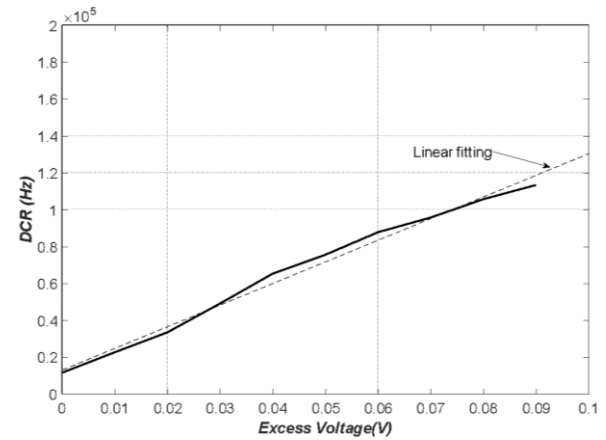


Figure 5. DCR vs. excess voltage. It was measured at intervals of 0.01 V. At room temperature, DCR linearly increases to the maximum 113.1 kHz.

finally organized count  $C_o$  and measurement time  $S_m$  were calculated as follows [4]:

$$DCR = \frac{C_o}{S_m} \quad (1)$$

In Figure. 5, it is capable of seeing the measured plot. DCR swiftly rises as the excess bias increases. As a result of the measurement, DCR ranged from minimum 11.5 kHz to maximum 113.1 kHz.

## 2.4 Photon Detection Probability measurement

PDP is a parameter that determines the photon sensitivity of SPAD, and proposed SPAD was measured under optical experiment setting. Since PDP varies in transmittance depending on the wavelength of the photon, it was tested with a fixed wavelength source to measure values at, in this work, target wavelength. The light source as a 405 nm laser is calibrated by using a Neutral Density (ND) filter and light flux controller. Thereby, the number of incident photons relative to AR is defined and the PDP is calculated as follows [5]:

Table 1 Comparison table

	[7]	[8]	[9]	[10]	[11]	This work
AR(Active region)	-	5 $\mu\text{m}$ (octagon)	12.4 $\mu\text{m}$ (circular)	20 $\mu\text{m}$	8 $\mu\text{m}$ (octagon)	5 $\mu\text{m}$
$V_{bd}/V_{ex}$	19.5 V / 3 V	9.52 V / 0.3 V	12.14 V / 0.4 V	9.9 V / 1.5 V	9.1 V / 0.4 V	10.75 V / 0.04 V
DCR(cps/ $\mu\text{m}^2$ )	1650 cps/ $\mu\text{m}^2$	138 kcps/ $\mu\text{m}^2$	629 cps/ $\mu\text{m}^2$ at 25°C 346 cps/ $\mu\text{m}^2$ at 15°C	2.8 kcps/ $\mu\text{m}^2$	15.6 kcps/ $\mu\text{m}^2$	286.3 cps/ $\mu\text{m}^2$
PDE	49.0 @ 480 nm	2.1 @ 440 nm	7.35 @ 560 nm	8 @ 470 nm	5.55 @ 420 nm	21.48 @ 405 nm

$$PDP = \delta \frac{CPS - DCR}{n_{incident}(\lambda) * \tau_m} \quad (2)$$

CPS is the number of output pulse peaks of SPAD when it was started to measure: DCR is defined before measurement:  $\tau_m$  is measurement time:  $\delta$  is ratio of the active area of SPAD:  $n_{incident}(\lambda)$  is the number of the photon calibrated by an optical source [6]. Result of the experiment is 21.48 % at room temperature.

### 3. Conclusion

This work report on the SPAD fabricated in the common CMOS process. The proposed design has a low breakdown voltage of about 11 V. DCR is 22.6 kHz at 0.04 V excess voltage. PDP are 21.48 % at 405 nm. Compared to Table 1, proposed SPAD can obtain a high PDE with a small size and a low breakdown voltage. They also can be improved sufficiently by integrating readout circuits. It shows the possibility of using it as a multi-monitoring system that has low power and micro-small.

As a result, the proposed SPAD showed strong advantages in low power consumption and small size. From these advantages, it is possible to install a comprehensive monitoring network system in nuclear power plants, and it will be used through additional verifications in harsh environments in the event of a severe accident. In addition, it may be used in a variety of fields, such as Fluorescence Lifetime Imaging (FLIM), light detection and ranging (LiDAR), positron emission tomography (PET) and Raman spectroscopy through performance development in the future.

Future work will evaluate radiation and temperature assuming a cold environment in the event of a nuclear accident and we plan to develop an advanced sensor interface in the form of on-chip by developing an array that is integrated with the readout stage.

### ACKNOWLEDGMENT

This work was supported in part by the Energy Technology Program of the Korea Institute of Energy Technology Evaluation and Planning (KETEP) granted financial resource from the Ministry of Trade, Industry & Energy, Republic of Korea (No. 20191510301290) and by Basic Science Research Program through the National Research Foundation of Korea (NRF) funded

by the Ministry of Science and ICT (2020M2A8A1000830).

### REFERENCES

- [1] S. Bose, H. Ouh, S. Sengupta and M. L. Johnston, "Parametric Study of p-n Junctions and Structures for CMOS-Integrated Single-Photon Avalanche Diodes," in IEEE Sensors Journal, vol. 18, no. 13, pp. 5291-5299, 1 July1, 2018, doi: 10.1109/JSEN.2018.2835762.
- [2] A. Gallivanoni, I. Rech and M. Ghioni, "Progress in Quenching Circuits for Single Photon Avalanche Diodes," in IEEE Transactions on Nuclear Science, vol. 57, no. 6, pp. 3815-3826, Dec. 2010, doi: 10.1109/TNS.2010.2074213.
- [3] V. Savuskan, M. Javitt, G. Visokolov, I. Brouk and Y. Nemirovsky, "Selecting Single Photon Avalanche Diode (SPAD) Passive-Quenching Resistance: An Approach," in IEEE Sensors Journal, vol. 13, no. 6, pp. 2322-2328, June 2013, doi: 10.1109/JSEN.2013.2253603.
- [4] Yue Xu, Tingchen Zhao, Ding Li, An accurate behavioral model for single-photon avalanche diode statistical performance simulation, Superlattices and Microstructures, Volume 113, 2018, Pages 635-643, ISSN 0749-6036, <https://doi.org/10.1016/j.spmi.2017.11.049>.
- [5] F. Gramuglia, M. -L. Wu, C. Bruschi, M. -J. Lee and E. Charbon, "A Low-Noise CMOS SPAD Pixel With 12.1 Ps SPTR and 3 Ns Dead Time," in IEEE Journal of Selected Topics in Quantum Electronics, vol. 28, no. 2, pp. 1-9, March-April 2022, Art no. 3800809, doi: 10.1109/JSTQE.2021.3088216.
- [6] H. Mahmoudi, S. S. K. Poushi, B. Steindl, M. Hofbauer and H. Zimmermann, "Optical and Electrical Characterization and Modeling of Photon Detection Probability in CMOS Single-Photon Avalanche Diodes," in IEEE Sensors Journal, vol. 21, no. 6, pp. 7572-7580, 15 March15, 2021, doi: 10.1109/JSEN.2021.3051365.
- [7] B. Bérubé et al., "Implementation Study of Single Photon Avalanche Diodes (SPAD) in 0.8  $\mu\text{m}$  HV CMOS Technology," in IEEE Transactions on Nuclear Science, vol. 62, no. 3, pp. 710-718, June 2015, doi: 10.1109/TNS.2015.2424852.
- [8] W. Jiang, Y. Chalich, R. Scott and M. J. Deen, "Time-Gated and Multi-Junction SPADs in Standard 65 nm CMOS Technology," in IEEE Sensors Journal, vol. 21, no. 10, pp. 12092-12103, 15 May15, 2021, doi: 10.1109/JSEN.2021.3063319
- [9] W. Jiang, R. Scott and M. J. Deen, "Improved Noise Performance of CMOS Poly Gate Single-Photon Avalanche Diodes," in IEEE Photonics Journal, vol. 14, no. 1, pp. 1-8, Feb. 2022, Art no. 6802208, doi: 10.1109/JPHOT.2021.3128055.
- [10] E. Charbon, H. Yoon and Y. Maruyama, "A Geiger mode APD fabricated in standard 65nm CMOS technology," 2013

IEEE International Electron Devices Meeting, 2013, pp. 27.5.1-27.5.4, doi: 10.1109/IEDM.2013.6724705.  
[11] Nolet, F.; Parent, S.; Roy, N.; Mercier, M.-O.; Charlebois, S.A.; Fontaine, R.; Pratte, J.-F. Quenching Circuit and SPAD Integrated in CMOS 65 nm with 7.8 ps FWHM Single Photon Timing Resolution. *Instruments* 2018, 2, 19. <https://doi.org/10.3390/instruments2040019>